Shape resonances in *K*-shell photodetachment of small size-selected clusters: Experiment and theory

N. Berrah,[1,*] R. C. Bilodeau,[1,2] J. D. Bozek,[2] I. Dumitriu,[1,2] D. Toffoli,[3] and R. R. Lucchese[3]
[1]*Department of Physics, Western Michigan University, Kalamazoo, Michigan 49008, USA*
[2]*Advanced Light Source Division, Lawrence Berkeley National Laboratory, Berkeley, California 94720, USA*
[3]*Department of Chemistry, Texas A&M University, College Station, Texas 77843-3255, USA*
(Received 25 April 2007; revised manuscript received 10 August 2007; published 11 October 2007)

K-shell photodetachment of size-selected B_2^- and B_3^- cluster anions has been measured and calculated. The experimental absolute photodetachment cross sections exhibit bound resonances below threshold and two shape resonances above the *K*-shell threshold. Similar results were obtained for all of the cationic products observed, B^+ and B_2^+ from B_2^-, as well as B^+, B_2^+, and B_3^+ from B_3^-. The overall agreement between measured and calculated photodetachment cross sections is very good. However, the theoretical study yielded additional bound resonances not observed in the experimental data.

DOI: 10.1103/PhysRevA.76.042709 PACS number(s): 32.80.Gc, 32.80.Hd

I. INTRODUCTION

Valence electron ionization studies in atomic, molecular, and cluster anions have been a quite prolific field of research for about 4 decades [1–3] using lasers. Because of the excess of negative charge compared to the neutral parent, electron correlation effects assume a prominent role in anions. Their investigations represent therefore an ideal testing ground for the ability of theoretical methods to model correlation phenomena. In general, compared to neutral systems or positive ions, studies on negative ions can potentially provide new information about electronic-structure and photoprocesses dynamics. Unlike neutral atoms and positive ions where the long-range Coulomb potential, proportional to r^{-1} dominates, in negative ions the attached electron moves in the field of a short-range potential (proportional to r^{-4}), leading thus to very different responses to electromagnetic radiation excitation in atoms [1], molecules [2,3], and clusters [4,5]. For example, in contrast to an infinite number of bound states supported by the long-range Coulomb potential for neutrals or positive ions, due to the short range binding potential, negative ions have only a finite number of states, often limited to only the fine structure of a single term. However, all negative ions possess unstable excited states which are embedded as resonances in the continuum associated with the free electron and the atom.

Inner-shell photodetachment studies of negative ions, however, have only recently been accessible as a result of improvements in synchrotron light sources. Inner-shell investigations of anions started simultaneously recently in two different research groups [6,7] and have triggered many new experimental studies [8,12] and considerable theoretical attention [13,15].

The behavior of the photodetachment cross sections of anions has been studied experimentally and theoretically [1–15] the past 4 decades in order to understand their structure and electronic decay dynamics revealed through various types of resonance structure. The progress in understanding negative ions structure and dynamics is to a large extent the result of the active interplay between experimental and theoretical studies [1–15] which allowed a rigorous identification of resonances and photodetachment thresholds, providing a clear picture of the anion electronic structure and dynamics.

Traditionally, resonances emerging from photodetachment or electron-atom scattering were divided into two classes; Feshbach and shape resonances are both important since they reveal the position of the states with respect to the parent atom. In the central-field independent-particle approximation, the atomic wave functions are determined by the attractive short range atomic potential $V(r) \sim 1/r^4$ and a repulsive centrifugal term $\sim l(l+1)/2r^2$; the sum of which gives an effective potential. Depending on the *shape* of the effective potential, the continuum wave function can display a resonance called shape resonance [16–18] because the photoelectron is trapped transitorily behind the centrifugal barrier. Moreover, these resonances are usually very short lived and should be considered as a one-electron phenomenon with energies above the energy of the parent atom. Contrary to shape resonances, Feshbach resonances [19,20] keep the excited electron bound for a long time compared to shape resonances and are found below the parent atom.

The classification and characterization of resonance structure have thus been important to determine not only for atomic and molecular anions [1–15] but also for neutral atoms and molecules in general [1–26], although the latter are not part of the scope of this work. As select examples, shape resonances are important in cold-atom scattering since "knowing the energy of a shape resonance leads very directly to an accurate scattering length for the corresponding potential" [21]. Furthermore, in the case of molecules, shape resonances [22–24] have been important due to the suggestion [25] that "the position of the resonance above threshold is related to the size of the molecule and thus could be used as a ruler to measure molecular dimensions" [26].

In this work, we report the experimental and theoretical study of *K*-shell photodetachment of the size-selected clusters B_2^- and B_3^- to explore possible resonance trends in small cluster systems. In addition, our measurements allow a

*nora.berrah@wmich.edu

qualitative measurement of the photofragmentation process in both B_2^- and B_3^-. The motivation for this work stems from the fact that although there is much sophisticated molecular and cluster anions laser photodetachment work [1–5], there is no information on inner-shell photodetachment and fragmentation of cluster and molecular anions to date, apart from a recent inner-valence photodetachment of CN^- [27].

Inner-shell photoexcitation or photodetachment offers the unique opportunity to study clusters and molecules with site specificity. While the interaction between photons and molecules or clusters is more intricate than the atomic case due to the more complicated electronic structure and coupling to nuclear motion in the polyatomic system, the site specificity of inner-shell excitation can make the complex reaction dynamics tractable as was found in this work.

This investigation has an impact in many areas of physics such as atomic, molecular, material, and astrophysics. In particular, it represents a direction in photoionization studies of small clusters, namely inner-shell photoexcitation of size-selected clusters. Moreover, the scalability of clusters and cluster-size dependent studies will probe the evolution of properties between the well-known and extensively studied single atoms or molecules and condensed matter systems. This makes small cluster studies unique for advancing fundamental understanding of the many-body problem. In addition, studies of the properties of ions are needed to better understand the "odd" species observed in the dilute plasmas on the outer atmosphere of stars and in interstellar space [28].

K-shell photodetachment of B_2^- consists of two mechanisms, ionization and dissociation, leading to three possible decay pathways:

$$\text{(a) } B_2^- + h\nu \rightarrow B_2^+ + 2e^-;$$

$$\text{(b) } B_2^- + h\nu \rightarrow B^+ + B + 2e^-;$$

$$\text{(c) } B_2^- + h\nu \rightarrow B^+ + B^- + e^-.$$

Our experimental technique allowed for only the measurement of cationic products, i.e., B_2^+ and B^+, but not of neutral B. In addition we attempted to detect B^-, but none was observed. Specifically, we report here on shape resonances observed in the parent B_2^+ (from B_2^-) or B_3^+ (from B_3^-) and photofragment B^+ or B_2^+ ions similar to the recent measurement and calculation results in the photodetachment of the monomer B^- resulting in B^+ [29]. Furthermore, we report the observation of resonances below threshold likely arising from sequential double Auger decay of the resonant states. In addition, we have determined absolute photodetachment cross sections for *K*-shell photodetachment of B_2^- leading to the loss of two electrons due to direct double ionization or single ionization followed by Auger decay. Moreover, photodetachment scattering dynamics calculations of B_2^- are presented which use the multichannel Schwinger variational method. The method is capable of accounting for both initial and final-state correlation effects through a configuration-interaction (CI) treatment of the anionic and final (neutral) target state, and of the interchannel coupling, through a limited-size close-coupling (CC) expansion of the stationary scattering wave function.

II. EXPERIMENTAL METHOD

The experiments were performed using the Ion-Photon beamline at beamline 10.0.1 at the Advanced Light Source. Details of the methodology to measure absolute photodetachment cross sections are described elsewhere [12,30]. Briefly, B_2^- and B_3^- ions produced using a cesium sputtering ion source were accelerated to about 8.56 keV producing beam currents of about 166 nA for B_2^- and 27 nA for B_3^- in the interaction region. These ions are likely to be vibrationally hot (900–1300 K). The ions were collinearly merged with the counterpropagating photon beam in a 30 cm long energy-tagged interaction region resulting in neutral (B, B_2, and B_3) as well as cationic (B^+, B_2^+, and B_3^+) products. Only the cationic B^+, B_2^+, and B_3^+ ions, produced by direct double photoionization and Auger decay, could be detected and were measured as a function of photon energy. Although we searched for anionic B^- fragments by reversing the magnetic field of the dispersing magnet, we did not observe any measurable signal. As for the B fragment, our present experimental configuration does not lend itself to allow the measurement of neutral species. Cations produced by photodetachment were deflected by a demerging magnetic field and counted using a multichannel plate based detector. The resulting signals were normalized to the primary B_2^-/B_3^- ion beam current and the incident photon flux. We note that due to the kinetic energy released (KER) in the fragmentation process, fragment ions are not collected with complete efficiency, and significant losses can be expected in the transport of the ions to the detector [27]. As a result, while the reported B_2^+ production cross section from B_2^- is reliable, the reported absolute cross sections for B^+ production from B_2^- photodetachment are lower limits and likely underestimated.

The photon energy was calibrated against accurately known absorption lines in Ar (4*s* line at 244.39 eV) [31] and SF_6 (two lines at 183.4 and 184.57 eV) [32]. Total uncertainty for the photon energy calibration, including Doppler correction, is estimated to be 65 meV [uncertainties are quoted to 1 standard deviation (SD) everywhere]. The data are corrected for the Doppler shift due to the momentum of the 8.5 keV ions. Note that the *x* axis of all the presented figures here correspond to the energy above the ground state of the neutral, i.e., the ion-frame photon energy minus the electron affinity of the respective atom or the molecule.

III. THEORETICAL METHODOLOGY

The stability of low-lying states of B_2^- were studied by Bruna *et al.* [33] using the multireference double configuration interaction (MRDCI) method. The B_2^- ground state is described by the configuration:

$$X\ {}^4\Sigma_g(1\sigma_g)^2(1\sigma_u)^2(2\sigma_g)^2(2\sigma_u)^2(3\sigma_g)^1(1\pi_u)^2(1\pi_g)^0(3\sigma_u)^0. \tag{1}$$

Bruna *et al.* [33] found a large set of stable anionic states [electron affinity (EA) >0]. The authors also provided a the-

TABLE I. *N*-electron initial state and $(N-1)$-electron states used in the multichannel scattering calculations for B_2^-.

State	MCCI vertical IP (eV)[a]	Important configurations[b]
	B_2^- ground state	
$X\ ^4\Sigma_g^-$		$0.89(3\sigma_g)^1(1\pi_u)^2$
		$0.05(2\sigma_u)^{-1}(3\sigma_g)^2(1\pi_u)^{-1}(1\pi_g)^1$
	B_2 *K*-shell excited target states	
$49\ ^3\Sigma_g^-$	197.10	$0.68(1\sigma_g)^{-1}$
		$0.15(1\sigma_u)^{-1}(2\sigma_u)^{-1}(3\sigma_g)^2$
$50\ ^3\Sigma_g^-$	197.50	$0.69(1\sigma_g)^{-1}$
		$0.12(1\sigma_u)^{-1}(2\sigma_u)^{-1}(3\sigma_g)^2$
$51\ ^3\Sigma_g^+$	198.12	$0.67(1\sigma_g)^{-1}$
		$0.13(1\sigma_u)^{-1}(2\sigma_u)^{-1}(3\sigma_g)^2$
$17\ ^5\Sigma_g^-$	196.37	$0.74(1\sigma_g)^{-1}$
		$0.11(1\sigma_u)^{-1}(1\pi_u)^{-1}(1\pi_g)^1$
$19\ ^3\Delta_g$	197.75	$0.71(1\sigma_g)^{-1}$
		$0.11(1\sigma_u)^{-1}(2\sigma_u)^{-1}(3\sigma_g)^1$
		$0.10(1\sigma_u)^{-1}(1\pi_u)^{-1}(1\pi_g)^1$
$49\ ^3\Sigma_u^-$	197.04	$0.70(1\sigma_u)^{-1}$
		$0.14(1\sigma_g)^{-1}(2\sigma_u)^{-1}(3\sigma_g)^2$
$50\ ^3\Sigma_u^-$	197.46	$0.69(1\sigma_u)^{-1}$
		$0.12(1\sigma_g)^{-1}(2\sigma_u)^{-1}(3\sigma_g)^2$
		$0.11(1\sigma_g)^{-1}(1\pi_u)^{-1}(1\pi_g)^1$
$51\ ^3\Sigma_u^+$	198.09	$0.67(1\sigma_u)^{-1}$
		$0.12(1\sigma_g)^{-1}(2\sigma_u)^{-1}(3\sigma_g)^2$
$11\ ^5\Sigma_u^-$	196.34	$0.75(1\sigma_u)^{-1}$
		$0.11(1\sigma_g)^{-1}(1\pi_u)^{-1}(1\pi_g)^1$
$19\ ^3\Delta_u$	197.71	$0.72(1\sigma_u)^{-1}$
		$0.11(1\sigma_g)^{-1}(2\sigma_u)^{-1}(3\sigma_g)^2$

[a]This work.
[b]Sum of the squares of the coefficients of the configuration state functions (CSFs) with the given configuration.

oretical value for the equilibrium bond length of the anion in its ground state of 3.081 a.u. (1.630 395 Å).

The multichannel Schwinger variational method with configuration interaction (MCCI) we use for calculating absolute total photodetachment cross sections of B_2^- has been described at length in the literature [34]. The one-electron scattering wave functions are obtained through the solution of a Lippman-Schwinger equation where additionally orthogonality constraints between the scattering wave function and bound molecular orbitals can be included. Dipole transition matrix elements between initial and final state channels are then computed using the Schwinger variational method with Padé corrections [34]. The single center expansion technique is used for expanding the bound and continuum orbitals [35]. Correlated wave functions for the initial (anionic B_2^-) and final (neutral B_2) target states are obtained through a numerical CI procedure using a set of natural orbitals obtained with the MOLPRO quantum chemistry package [36].

Several multiconfigurational self-consistent field (MCSCF) calculations following a restricted-open Hartree-Fock (ROHF) calculation on the $X\ ^4\Sigma_g^-$ ground state of B_2^- have been performed in order to select the optimal set of molecular orbitals to be used in the subsequent scattering calculations. The augmented correlation-consistent valence triple zeta basis set (aug-cc-pVTZ) of Dunning was used [37]. With this basis set, we obtained a SCF energy of −49.17 136 789 a.u. at the equilibrium bond length of the anion of 3.081 a.u. [33]. The natural orbitals used in the numerical CI procedure were obtained after a MCSCF calculation with all the orbitals listed in Eq. (1) included in the active space, with the exception of the core B 1*s* orbitals, which were excluded but optimized. The MCSCF energy obtained was −49.245 304 88 a.u.

The numerical CI calculations were performed with all the electrons active, with an active space as given by Eq. (1). Restrictions were imposed on the number of excitations to virtual orbitals in such a way that a maximum of two-electron excitations were allowed for the computation of the B_2^- ground state, and only single excitations were allowed for the CI expansion of the final B_2 neutral target states. The bound molecular and scattering orbitals were partial-wave expanded up to $l_{max}=60$.

Assuming the validity of the Koopman's picture, a hole in either the $1\sigma_g$ or $1\sigma_u$ orbital of B_2^- gives rise to ten terms which are listed in Table I. For each of the target states, Table I lists the calculated vertical CI ionization (detachment) potential (IP) along with the principal configurations. A close-coupling (CC) expansion of the stationary scattering wave function restricted to *K*-shell single-hole channels would involve a ten-channel calculation. In order to keep the size of the CC expansion tractable only a subset of neutral target states which have a large (>0.06) spectroscopic intensity factor (SIFs) were retained in the CC expansion. The target states included in the multichannel scattering calculations were the $49\ ^3\Sigma_g^-$, $17\ ^5\Sigma_g^-$, $49\ ^3\Sigma_u^-$, and $11\ ^5\Sigma_u^-$ states. We additionally included the ground state of B_2 for the purpose of a qualitative analysis of the occurrence of resonances below threshold, giving a five channel (5-MCCI) scattering calculation.

IV. RESULTS AND DISCUSSION

Experimental absolute photodetachment cross sections of B^+ and B_2^+ from B_2^- taken at low photon resolution (390 meV bandwidth) in the region of the B 1*s* ionization threshold are shown in Fig. 1. Also shown in the figure (top spectrum) are B^+ data (filled black circles) resulting from Auger decay of 1*s* photodetachment of atomic B^- [29] to allow comparison with the 1*s* photodetachment of B_2^-. The blue squares in the B_2^+ spectrum correspond to absolute cross section measurements used to scale the spectral data. The three spectra are vertically offset with respect to each other for presentation. From Fig. 1, one can observe a very close similarity between the two dimer spectra $B_2^- \rightarrow B_2^+$ and $B_2^- \rightarrow B^+$ and a close correspondence with atomic spectrum, $B^- \rightarrow B^+$. Absolute cross sections of 0.445 (86) Mb, 0.396(81), and 0.463 (93) correspond to the average of several measurements at 187.318, 192.732, and 196.241 eV, respectively. The uncertainty in these measured absolute cross sections is about 23%, which is typical for merged ion-photon beam experiments [6,10]. Furthermore, branching ra-

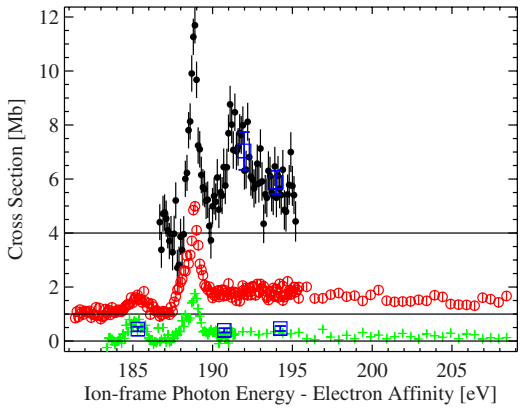

FIG. 1. (Color online) *K*-shell photodetachment of B^- (top spectrum [29]), and B_2^- (middle and bottom spectra). Energies have been shifted by the respective electron affinities of the target ions. The middle spectrum corresponds to the B^+ fragment while the bottom one corresponds to the B_2^+ parent. Note that KER effects result in significant losses of the B^+ fragment and these cross sections are likely underestimated. (See text for details.)

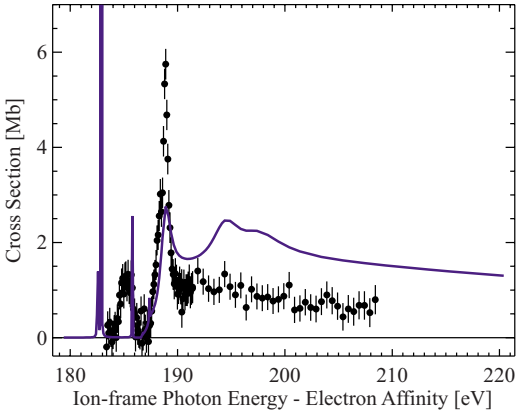

FIG. 2. (Color online) Comparison between the measured two-electron detachment ($B^+ + B_2^+$) yields from B_2^- (filled circles) and theoretical 5C-MCCI results for B_2^- single electron photodetachment (solid line). The energy scale has been shifted by the electron affinity of B_2^- (2.0 eV). Note that the experimental cross section scale ignores potential B^+ loss due to KER effects.

tio measurements [11] between B^+ and B_2^+ ions allowed absolute scaling of the B^+ data. Note that both spectra have been shifted in energy by their respective electron affinities (0.28 eV for B [38] and 2.0 eV for B_2 [33]) as indicated by the *x*-axis label resulting in the alignment of the prominent peaks in the spectrum. The first peak in the atomic $B^- \rightarrow B^+$ cross section curve corresponds to three unresolved shape resonances (not resolved with the 390 meV photon bandwidth used here) just above the $1s2s^22p^2(^4P)$ threshold, while the second broad structure corresponds to the expected turn-on of the *K*-shell photodetachment at the $1s2s^22P^2(^4P)$ threshold [29].

To aid in the interpretation of the photodetachment of B_2^-, we compare the sum of the cationic production ($B_2^+ + B^+$) with the 5-MCCI calculations of photodetachment cross section leading to neutral B_2. This qualitative comparison is reasonable, since all K-hole excited states of B_2 are autoionizing states which will quickly decay to B_2^+. The comparison between experimental and theoretical results is shown in Fig. 2. The theoretical curve is shifted by −7.84 eV, a value obtained by assuming that the first core-hole excited state of B_2 ($11\ ^5\Sigma_u^-$ calculated to have vertical ionization potential of 196.34 eV) should have the same energy (best estimate value of 188.5 eV) as the $^4P^e$ state of atomic B [29]. The shift applied to the theoretical data is quite reasonable in view of the limited set of molecular orbitals included in the numerical CI calculations and the truncated partial-wave expansion used. The energy shift applied compares with typical ones applied in *K*-shell photoionization of small-size molecules such as C_2H_2 [39]. The shifted theoretical curve agrees qualitatively very well with the experimental data sets. Although a strict quantitative comparison between calculated photodetachment cross section and measured B_2^+ cross section is not valid, we can still gain a qualitative understanding of the experimental spectrum from the theoretical results. The first two calculated spectral features below threshold are interpreted as due to $1\sigma_u \rightarrow 3\sigma_g$ and $1\sigma_g \rightarrow 1\pi_u$ discrete excitations but are not observed. Another one centered at about 187.2 eV is interpreted as a discrete $1\sigma_u \rightarrow 1\pi_g$ resonant excitation having a counterpart in the experimental spectrum. This resonance can be observed in the positive ion formation channel due to double-Auger decay of the excited state. Because of the significant difference in relative strengths between sequential and simultaneous double Auger processes, this is likely a sequential decay process [40]. We should note that agreement between calculated and experimental intensities for the below threshold features can be expected to be qualitative at best for several reasons: (a) already in the fixed-nuclei approximation the relevant decay channels are not included in the CC expansion of the wave function; (b) the features are likely further broadened by rovibrational excitations of the inner-shell excited state (which were not included in the calculation which is not sensitive to these excitations), as was observed in the NEXAFS spectra of other diatomic molecules such as CO [41] and N_2 [42] which have preedge peaks that are several hundred meV wide; and (c) there are decay channels for the below threshold resonances that can lead to neutral products and would thus not be observed in the present experiments. The broadening of the experimentally measured resonance is also partly due to the experimental spectral bandwidth.

Above threshold the calculated cross section exhibits two main resonant enhancements. The peak just above the threshold at about 190.8 eV is a signature of overlapping shape-resonances in the $1\sigma_u \rightarrow k\pi_g$ and $1\sigma_g \rightarrow k\pi_u$ continua with a total symmetry of $^4\Pi_u$ in the $11\ ^5\Sigma_u^-$ and $17\ ^5\Sigma_g^-$ channels, respectively. The calculated features have a nice counterpart in the experimental profile. The predicted resonant peak at about 196 eV and the shoulder at 198 eV are interpreted as shape resonances in the $1\ \sigma_g \rightarrow k\sigma_u$ continuum with a total symmetry of $^4\Sigma_u$ in the $17\ ^5\Sigma_g^-$ and $49\ ^3\Sigma_g^-$ channels which, however, are not observed as distinct peaks in the experimental spectra. Instead, the experimental cross section exhibits a spread out enhancement to well above threshold.

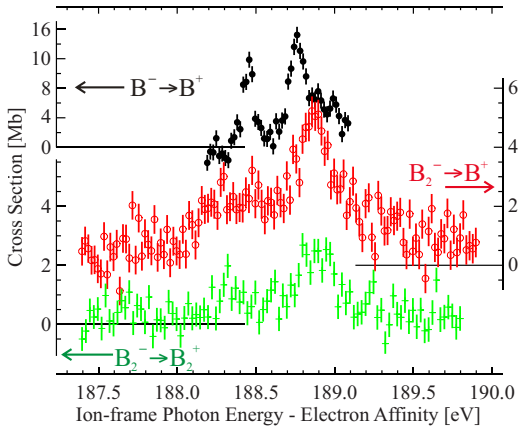

FIG. 3. (Color online) High-resolution *K*-shell photodetachment measurements of B^- (top spectrum) [29] and of B_2^- (middle and bottom spectra). The two structures observed are shape resonances. The energies have been shifted by the respective electron affinities of the target ions.

To further compare and contrast the molecular (B_2^+ and B^+ from B_2^-) cross sections in the region of the shape resonances with the atomic (B^+ from B^-) ones, we display in Fig. 3 higher resolution *K*-shell photodetachment measurements (100 meV bandwidth) of the B^- (top spectrum) and B_2^- (B^+ middle and B_2^+ bottom spectra) anion between 187 and 190 eV. In the $B^- \rightarrow B^+$ case, the two clearly observed peaks are $1s2s^22p^3$ (^3D and ^3S, respectively) shape resonances while the ^3P weaker resonance forms a hump to the high energy side of the ^3S resonance [29]. The middle spectrum shows the B^+ fragment production from B_2^- photodetachment over the energy range of the second structure shown in the middle of Fig. 1 which can be assigned to the two $1\sigma_u \rightarrow k\pi_g$ and $1\sigma_g \rightarrow k\pi_u$ shape resonances theoretically predicted at about 189 eV. This finding thus *mirrors* the atomic photodetachment results. The lower spectrum, which shows the B_2^+ production from B_2^- photodetachment over the same energy range, is similarly resolved into two structures, which again we assign as to consist of the $1\sigma_u \rightarrow k\pi_g$ and $1\sigma_g \rightarrow k\pi_u$ shape resonances.

The close similarity between the atomic and molecular spectra is initially rather surprising since more intricate spectra might be expected from the more complicated molecular system. However, since negative ions do not support many bound states (due to the lack of long range Coulomb interaction) the similarities of the molecular spectra with the atomic spectrum, along with their simplicity, might be understood due to the fact that anion's relaxation is different than the neutral or ionic case which support many bound states. In addition, *K*-shell photoionization or detachment is site specific, and thus produces atomiclike spectra inherently.

Similar trends are observed for the *K*-shell photodetachment of B_3^-, as shown in Fig. 4, albeit with lower statistics than that for the *K*-shell photodetachment of B_2^-. (Note again that these are also shifted for electron affinity. The EA of B_3^- is not known and an approximate value of 2 eV has been assumed here.) The measurements were carried out with 400 meV photon bandwidth and the curves are further

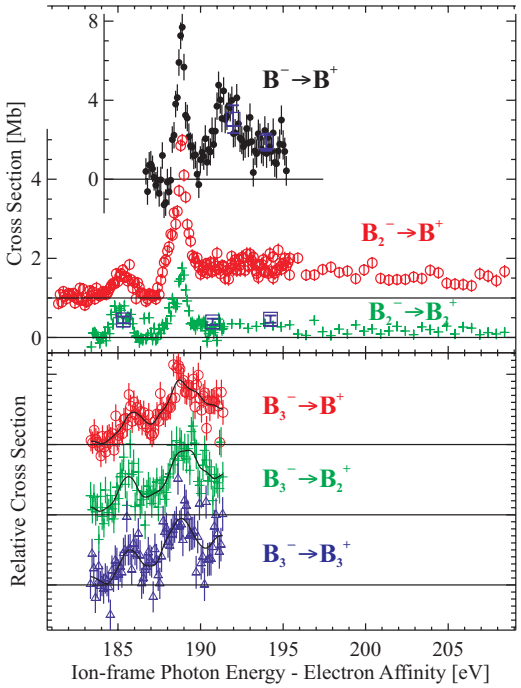

FIG. 4. (Color online) Comparison among *K*-shell photodetachment of B^- (spectrum in inset, top panel) [29], B_2^- (middle two spectra in top panel), and B_3^- (three spectra in bottom panel). (See text for details.) The energies have been shifted by the respective electron affinities of the target ions.

Gaussian-smoothed over 700 meV to smooth out statistical variations due to the weak signal. The top panel reproduces the results from Fig. 1 while the lower panel consists of relative cross sections of the fragment cations resulting from the photodetachment of B_3^-. The latter process produces B^+, B_2^+, and B_3^+ exhibiting below threshold (~187 eV) a structure which might be due to a discrete excitation while above threshold for each channel one can observe a structure that may be due to a shape resonance. Thus the trimer case also exhibits simple spectra, similar to the dimer and monomer. Here also the broadening of the structures may be due to vibrational excitations. Further optimization of the experimental conditions will be required to increase the signal and resolution of these spectra for further studies.

V. CONCLUSION

The present work has explored for the first time *K*-shell photodetachment of small size-selected clusters; B_2^- and B_3^-, and compared it with the same process for the monomer. The B_2^- measurements have been compared with theoretical multichannel scattering calculations for the *K*-shell total photodetachment cross section. The observed photodetachment cross sections exhibit a bound resonance below threshold probably due to sequential double Auger decay and two shape resonances above the *K*-shell threshold due to single Auger decay in the detected B_2^+ parent as well as a B^+ fragment produced by dissociation. The overall agreement between measurements and calculations is good. Further-

more, the measurements are strikingly similar to the *K*-shell photodetachment of the monomer B^-. A similar trend is also observed, albeit with lower statistics, in the case of the photodetachment of B_3^-. This work demonstrates the feasibility of 1*s* photodetachment studies of small cluster anions, studies that could be applied to size-selected clusters, monoatomic and mixed, of other materials.

ACKNOWLEDGMENTS

This work was supported by DOE, Office of Science, Basic Energy Science, Chemical, Geoscience and Biological divisions. We thank T. Rescigno, B. McCurdy, and T. Gorczyca for useful discussions. R.R.L. and D.T. acknowledge support from the Robert A. Welch Foundation under Grant No. A-1020.

[1] T. Andersen, Phys. Rep. **394**, 157 (2004), and references therein.
[2] T. Taylor *et al.*, J. Chem. Phys. **115**, 4620 (2001), and references therein.
[3] T. M. Ramond *et al.*, J. Mol. Spectrosc. **216**, 1 (2002), and references therein.
[4] A. E. Bragg, J. R. R. Verlet, A. Kammrath, and D. M. Neumark, J. Chem. Phys. **121**, 3515 (2004).
[5] N. Pontius, P. S. Bechthold, M. Neeb, and W. Eberhard, Phys. Rev. Lett. **84**, 1132 (2000).
[6] H. Kjeldsen, P. Andersen, F. Kristensen, and T. J. Andersen, J. Phys. B **34**, L353 (2001).
[7] N. Berrah *et al.*, Phys. Rev. Lett. **87**, 253002 (2001), and references therein.
[8] N. Berrah *et al.*, Phys. Scr., T **T110**, 51 (2004), and references therein.
[9] H. Kjeldsen, F. Folkmann, T. S. Jacobsen, and J. B. West, Phys. Rev. A **69**, 050501(R) (2004), and references therein.
[10] A. Aguilar *et al.*, Phys. Rev. A **69**, 022711 (2004), and references therein.
[11] R. C. Bilodeau, J. D. Bozek, N. D. Gibson, C. W. Walter, G. D. Ackerman, I. Dumitriu, and N. Berrah, Phys. Rev. Lett. **95**, 083001 (2005), and references therein.
[12] C. W. Walter, N. D. Gibson, R. C. Bilodeau, N. Berrah, J. D. Bozek, G. D. Ackerman, and A. Aguilar, Phys. Rev. A **73**, 062702 (2006).
[13] J. L. Sanz-Vicario, E. Lindroth, and N. Brandefelt, Phys. Rev. A **66**, 052713 (2002).
[14] H.-L. Zhou, S. T. Manson, L. Voky, A. Hibbert, and N. Feautrier, Phys. Rev. A **64**, 012714 (2001).
[15] T. W. Gorczyca, O. Zatsarinny, H. L. Zhou, S. T. Manson, Z. Felfli, and A. Z. Msezane, Phys. Rev. A **68**, 050703(R) (2003), and references therein.
[16] S. J. Buckman and C. W. Clark, Rev. Mod. Phys. **66**, 539 (1994).
[17] U. Fano and J. W. Cooper, Rev. Mod. Phys. **40**, 441 (1968).
[18] N. Berrah *et al.*, Phys. Rev. Lett. **87**, 253002 (2001); H. Kjeldsen *et al.*, J. Phys. B **34** L353 (2001); C. W. Walter, N. D. Gibson, R. C. Bilodeau, N. Berrah, J. D. Bozek, G. D. Ackerman, and A. Aguilar, Phys. Rev. A **73**, 062702 (2006).
[19] R. C. Bilodeau, J. D. Bozek, A. Aguilar, G. D. Ackerman, G. Turri, and N. Berrah, Phys. Rev. Lett. **93**, 193001 (2004), and references therein.
[20] H. Kjeldsen, F. Folkmann, T. S. Jacobsen, and J. B. West, Phys. Rev. A **69**, 050501(R) (2004).
[21] H. M. J. M. Boesten, C. C. Tsai, B. J. Verhaar, and D. J. Heinzen, Phys. Rev. Lett. **77**, 5194 (1996).
[22] J. Dehmer and D. Dill, *Electron-Molecule and Photon-Molecules Collisions*, edited by T. Rescigno, V. McKoy, and B. Schneider (Plenum, New York, 1979), pp. 225–265.
[23] J. Dehmer and D. Dill, Phys. Rev. Lett. **35**, 213 (1975).
[24] W. C. Stolte, D. L. Hansen, M. N. Piancastelli, I. Dominguez Lopez, A. Rizvi, O. Hemmers, H. Wang, A. S. Schlachter, M. S. Lubell, and D. W. Lindle, Phys. Rev. Lett. **86**, 4504 (2001).
[25] A. P. Hitchcock *et al.*, J. Chem. Phys. **80**, 3927 (1984); **81**, 4906 (1984); J. Stohr, F. Sette, and A. L. Johnson, Phys. Rev. Lett. **53**, 1684 (1984).
[26] T. D. Thomas, N. Berrah, J. Bozek, T. X. Carroll, J. Hahne, T. Karlsen, E. Kukk, and L. J. Saethre, Phys. Rev. Lett. **82**, 1120 (1999).
[27] R. C. Bilodeau *et al.*, Chem. Phys. Lett. **426**, 237 (2006).
[28] M. C. McCarthy *et al.*, Astrophys. J. **652**, L141 (2006).
[29] N. Berrah, R. C. Bilodeau, I. Dumitriu, J. D. Bozek, G. D. Ackerman, O. T. Zatsarinny, and T. W. Gorczyca, Phys. Rev. A (to be published).
[30] R. C. Bilodeau, J. D. Bozek, G. D. Ackerman, A. Aguilar, and N. Berrah, Phys. Rev. A **73**, 034701 (2006).
[31] G. C. King *et al.*, J. Phys. B **10**, 2479 (1977).
[32] E. Hudson, D. A. Shirley, M. Domke, G. Remmers, A. Puschmann, T. Mandel, C. Xue, and G. Kaindl, Phys. Rev. A **47**, 361 (1993).
[33] P. J. Bruna and J. S. Wright, J. Phys. B **23**, 2197S (1990).
[34] R. E. Stratmann and R. R. Lucchese, J. Chem. Phys. **102**, 8493 (1995).
[35] F. A. Gianturco *et al.*, *Electron Collisions with Molecules, Clusters, and Surfaces*, edited by H. Ehrhardt and L. A. Morgan (Plenum, New York, 1994), p. 71.
[36] R. D. Amos *et al.*, MOLPRO, version 2000.1 (University of Birmingham, Birmingham, 2000).
[37] T. H. Dunning, J. Chem. Phys. **90**, 1007 (1989).
[38] M. Scheer, R. C. Bilodeau, and H. K. Haugen, Phys. Rev. Lett. **80**, 2562 (1998).
[39] P. Lin and R. R. Lucchese, J. Chem. Phys. **113**, 1843 (2000).
[40] R. C. Bilodeau, J. D. Bozek, A. Aguilar, G. D. Ackerman, G. Turri, and N. Berrah, Phys. Rev. Lett. **93**, 193001 (2004), and references therein.
[41] S. K. Botting and R. R. Lucchese, Phys. Rev. A **56**, 3666 (1997).
[42] C. T. Chen, Y. Ma, and F. Sette, Phys. Rev. A **40**, 6737 (1989).